ELSEVIER

Computer-Aided Design xx (2003) xxx–xxx

COMPUTER-AIDED DESIGN

www.elsevier.com/locate/cad

Parametric representation of a surface pencil with a common spatial geodesic

Guo-Jin Wang[a], Kai Tang[b,*], Chiew-Lan Tai[c]

[a]*State Key Lab of CAD and CG, Department of Mathematics, Zhejiang University, Hangzhou 310027, China*
[b]*Department of Mechanical Engineering, Hong Kong University of Science and Technology, Clear Water Bay, Kowloon, Hong Kong, China*
[c]*Department of Computer Science, Hong Kong University of Science and Technology, Hong Kong, China*

Received 16 April 2003; received in revised form 30 May 2003; accepted 1 June 2003

Abstract

In this paper, we study the problem of constructing a family of surfaces from a given spatial geodesic curve. We derive a parametric representation for a surface pencil whose members share the same geodesic curve as an isoparametric curve. By utilizing the Frenet trihedron frame along the given geodesic, we express the surface pencil as a linear combination of the components of this local coordinate frame, and derive the necessary and sufficient conditions for the coefficients to satisfy both the geodesic and the isoparametric requirements. We illustrate and verify the method by finding exact surface pencil formulations for some simple surfaces, such as surfaces of revolution and ruled surfaces. Finally, we demonstrate the use of this method in a garment design application.

Keywords: Surface pencil; Geodesic; Frenet frame; Surface flattening

1. Introduction

Geodesic on a surface is an intrinsic geometric feature that plays an important role in a diversity of applications. Geometrically, a geodesic on a surface is an embedded simple curve on the surface such that for any two points on the curve the portion of the curve connecting them is also the shortest path between them on the surface. Many geometric operations are inherently related to geodesics. For instance, when a developable surface is flattened into a planar figure (with no distortion), any geodesic on it will be mapped to a straight line in the planar figure [10]. Thus, to flatten an arbitrary non-developable surface with as little distortion as possible, a good algorithm should try to preserve the geodesic curvatures on the surface [2,3]. Geodesic method also finds its applications in computer vision and image processing, such as in object segmentation [6,7,26] and multi-scale image analysis [22,28]. The concept of geodesic also finds its place in various industrial applications, such as tent manufacturing, cutting and painting path, fiberglass tape windings in pipe manufacturing, textile manufacturing [4,5,12,14–17,35].

Traditional fundamental research in geodesics concentrated on finding and characterizing geodesics on analytical curved surfaces [31]. As the computer becomes increasingly more powerful, and discretized models become more prevalent in geometric modeling, discrete geodesics have also been gaining attention. Over the last decade there has been a flush of research results on how to efficiently compute geodesics on discretized surfaces (i.e. polyhedra or grid-based systems) [1,8,11,13,18–30,32]. Regardless of the representation of the surface, most existing work on geodesics can be viewed as ‘forward analysis’: given a surface, how to find a geodesic or a structure of geodesics.

In this paper, we study the reverse problem, or ‘backward synthesis’: given a 3D curve, how to characterize those surfaces that possess this curve as a common geodesic. This is a reverse engineering problem. We use an example in shoe design to illustrate potential applications of this problem. Fig. 1 shows a model of a women’s shoe, which is usually represented by one or several free-form B-spline surfaces. On the shoe, there is one important characteristic curve called the *girth*, which more or less measures the width and height of the shoe. Given a particular model and

* Corresponding author.
E-mail address: mektang@ust.hk (K. Tang).

0010-4485/03/$ - see front matter © 2003 Elsevier Ltd. All rights reserved.
doi:10.1016/S0010-4485(03)00117-9

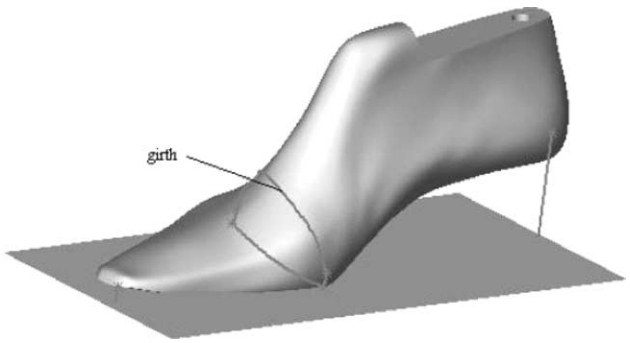

Fig. 1. A shoe surface model with its girth curve.

the nominal size of the shoe (say USA women's size 8), the girth is usually fixed, while the shape of the shoe changes frequently to suit various design intents, e.g. the fashion. A common practice in shoe manufacturing industry is to require that, when the shoe's surface is flattened to the plane, the girth should be mapped to a straight or near-straight line with minimum flattening distortion. This implies that the girth is preferred to be a geodesic on the shoe's surface.

Given a 3D parametric curve $\mathbf{r}(s)$, $0 \le s \le L$, we call $\mathbf{r}(s)$ an *isogeodesic* of a surface $\mathbf{P}$ if it is both a geodesic and an isoparametric curve on $\mathbf{P}$; in other words, $\mathbf{P}$ can be expressed as a parametric representation $\mathbf{P}(s,t)$ and there exists a parameter t_0 such that $\mathbf{r}(s) = \mathbf{P}(s,t_0)$, $0 \le s \le L$. The objective of study in this paper is to establish the correct parametric representation of $\mathbf{P}(s,t)$ for a given $\mathbf{r}(s)$. In Section 2, by utilizing the Frenet trihedron frame from differential geometry, we derive the necessary and sufficient conditions for the correct parametric representation of the surface $\mathbf{P}(s,t)$ when the parameter s is the arc length of the curve $\mathbf{r}(s)$. The basic idea is to represent $\mathbf{P}(s,t)$ as a linear combination of the three vector functions $\mathbf{T}(s)$, $\mathbf{N}(s)$, and $\mathbf{B}(s)$, which are the tangent vector, the principal normal, and the binormal of $\mathbf{r}(s)$, respectively, and find the necessary constraints on the coefficients of these vectors so that both the geodesic and isoparametric requirements are met. Since arc-length parametrization is impractical, in Section 3 we also give the parametric representation of the surface pencil for the case when the given geodesic curve is arbitrarily parametrized. To verify the formulae derived in Sections 2 and 3, and also for illustration purpose of the application of an isogeodesic surface pencil in geometric design, in Section 4 we choose some simple yet representative geodesic curves $\mathbf{r}(s)$ and determine the exact corresponding surface pencils that not only share the common geodesic but also contain certain known geometric features such as cylinders, surface of revolution, and ruled surfaces. Finally, as a practical example, an application of the isogeodesic surface pencil in garment design is presented in Section 5. We conclude the paper in Section 6 with some pointers to possible future research in this area.

2. Parametric representations of a geodesic surface pencil

Suppose we are given a spatial parametric curve

$$C: \ \mathbf{r} = \mathbf{r}(s), \qquad 0 \le s \le L, \tag{2.1}$$

in which s is the arc length, and $\mathbf{r}(s)$ has third derivatives. We assume that $\mathbf{r}''(s) \ne 0$, $0 \le s \le L$, because otherwise the curve is a straight line segment or the principal normal is undefined at some points on the curve.

Let $\mathbf{T}(s)$, $\mathbf{N}(s)$, and $\mathbf{B}(s)$ be the tangent, principal normal, and binormal vectors of the curve C, respectively; and let $\kappa(s)$ and $\tau(s)$ be the curvature and the torsion, respectively. The parametric surface $\mathbf{P}(s,t) : [0,L] \times [0,T] \to \Re^3$ is defined based on the given curve $\mathbf{r}(s)$ and the local coordinate frame defined by $\mathbf{T}(s)$, $\mathbf{N}(s)$, and $\mathbf{B}(s)$ as follows (see Fig. 2):

$$\mathbf{P}(s,t) = \mathbf{r}(s) + (u(s,t), v(s,t), w(s,t)) \begin{pmatrix} \mathbf{T}(s) \\ \mathbf{N}(s) \\ \mathbf{B}(s) \end{pmatrix}, \tag{2.2}$$

$$0 \le s \le L, \ 0 \le t \le T,$$

where $u(s,t)$, $v(s,t)$ and $w(s,t)$ are all C^1 functions. If the parameter t is seen as the time, the functions $u(s,t)$, $v(s,t)$ and $w(s,t)$ can then be viewed as directed marching distances of a point unit in the time t in the direction $\mathbf{T}(s)$, $\mathbf{N}(s)$, and $\mathbf{B}(s)$, respectively, and the position vector $\mathbf{r}(s)$ is seen as the initial location of this point unit. Here the values of the functions $u(s,t)$, $v(s,t)$, and $w(s,t)$ indicate, respectively, the extension-like, flexion-like, and retortion-like effects, by the point unit through the time t, starting from $\mathbf{r}(s)$. Hence in this paper we call $u(s,t)$, $v(s,t)$, and $w(s,t)$ the *marching-scale functions* in the directions $\mathbf{T}(s)$, $\mathbf{N}(s)$, and $\mathbf{B}(s)$, respectively.

Our goal is to find the necessary and sufficient conditions for which the curve C is a geodesic on the surface $\mathbf{P}(s,t)$. First, since the curve C is an isogeodesic on the surface

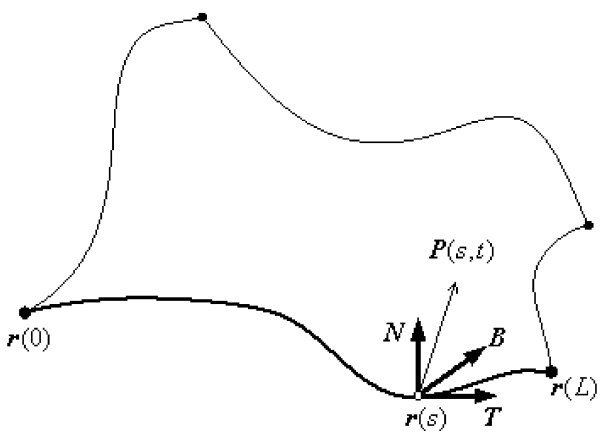

Fig. 2. Generating a surface $\mathbf{P}(s,t)$ based on the Frenet frame of the curve $\mathbf{r}(s)$.

$\mathbf{P}(s,t)$, there exists a parameter $t=t_0\in[0,T]$ such that $\mathbf{P}(s,t_0)=\mathbf{r}(s)$, $0\le s\le L$, that is,

$$u(s,t_0)=v(s,t_0)=w(s,t_0)\equiv 0,\quad t_0\in[0,T],0\le s\le L. \tag{2.3}$$

Secondly, according to the geodesic theory [31], the curve C is a geodesic on the surface $\mathbf{P}(s,t)$ if and only if at any point on the curve C the principal normal $\mathbf{N}(s)$ to the curve and the normal $\mathbf{n}(s,t_0)$ to the surface $\mathbf{P}(s,t)$ are parallel to each other. The normal $\mathbf{n}(s,t_0)$ can be computed by taking the cross product of the partial differentials; that is, based on the following derivation using the Serret–Frenet formula

$$\frac{\partial\mathbf{P}(s,t)}{\partial s}=\mathbf{T}(s)+(u(s,t),v(s,t),w(s,t))\begin{pmatrix}0&\kappa(s)&0\\-\kappa(s)&0&\tau(s)\\0&-\tau(s)&0\end{pmatrix}\times\begin{pmatrix}\mathbf{T}(s)\\\mathbf{N}(s)\\\mathbf{B}(s)\end{pmatrix}+\left(\frac{\partial u(s,t)}{\partial s},\frac{\partial v(s,t)}{\partial s},\frac{\partial w(s,t)}{\partial s}\right)\begin{pmatrix}\mathbf{T}(s)\\\mathbf{N}(s)\\\mathbf{B}(s)\end{pmatrix}$$

and

$$\frac{\partial\mathbf{P}(s,t)}{\partial t}=(\mathbf{T}(s),\mathbf{N}(s),\mathbf{B}(s))\begin{pmatrix}\frac{\partial u(s,t)}{\partial t}\\\frac{\partial v(s,t)}{\partial t}\\\frac{\partial w(s,t)}{\partial t}\end{pmatrix},$$

the normal vector can be expressed as

$$\mathbf{n}(s,t)=\frac{\partial\mathbf{P}(s,t)}{\partial s}\times\frac{\partial\mathbf{P}(s,t)}{\partial t}=\left(1-v(s,t)\kappa(s)+\frac{\partial u(s,t)}{\partial s},u(s,t)\kappa(s)-w(s,t)\tau(s)+\frac{\partial v(s,t)}{\partial s},v(s,t)\tau(s)+\frac{\partial w(s,t)}{\partial s}\right)\times\begin{pmatrix}0&\mathbf{B}(s)&-\mathbf{N}(s)\\-\mathbf{B}(s)&0&\mathbf{T}(s)\\\mathbf{N}(s)&-\mathbf{T}(s)&0\end{pmatrix}\begin{pmatrix}\frac{\partial u(s,t)}{\partial t}\\\frac{\partial v(s,t)}{\partial t}\\\frac{\partial w(s,t)}{\partial t}\end{pmatrix}.$$

Thus, we get

$$\mathbf{n}(s,t_0)=\phi_1(s,t_0)\mathbf{T}(s)+\phi_2(s,t_0)\mathbf{N}(s)+\phi_3(s,t_0)\mathbf{B}(s),$$

where

$$\phi_1(s,t_0)=\frac{\partial v(s,t_0)}{\partial s}\frac{\partial w(s,t_0)}{\partial t}-\frac{\partial w(s,t_0)}{\partial s}\frac{\partial v(s,t_0)}{\partial t},$$

$$\phi_2(s,t_0)=-\left(1+\frac{\partial u(s,t_0)}{\partial s}\right)\frac{\partial w(s,t_0)}{\partial t}+\frac{\partial w(s,t_0)}{\partial s}\frac{\partial u(s,t_0)}{\partial t},$$

$$\phi_3(s,t_0)=\left(1+\frac{\partial u(s,t_0)}{\partial s}\right)\frac{\partial v(s,t_0)}{\partial t}-\frac{\partial v(s,t_0)}{\partial s}\frac{\partial u(s,t_0)}{\partial t}.$$

Since

$$\mathbf{N}(s)=\frac{1}{\kappa(s)}\frac{\mathrm{d}^2\mathbf{r}(s)}{\mathrm{d}s^2},$$

we know that $\mathbf{N}(s)\|\mathbf{n}(s,t_0)$, $0\le s\le L$, if and only if

$$\begin{aligned}&\phi_1(s,t_0)=\phi_3(s,t_0)\equiv 0,\\&\phi_2(s,t_0)\ne 0,\ 0\le s\le L,\ 0\le t_0\le T.\end{aligned} \tag{2.4}$$

Combining the conditions (2.3) and (2.4), we have found the necessary and sufficient conditions for the surface $\mathbf{P}(s,t)$ to have the curve C as an isogeodesic.

To distinguish from other parametric surfaces that also have the curve C as a geodesic, we call the set of surfaces defined by Eqs. (2.2)–(2.4) an *isogeodesic surface pencil*, since the common geodesic is also an isoparametric curve on these surfaces. Any surface $\mathbf{P}(s,t)$ defined by Eq. (2.2) and satisfying Eqs. (2.3) and (2.4) is a member of this pencil. For the purposes of simplification and better analysis, next we study the case when the marching-scale functions $u(s,t)$, $v(s,t)$, and $w(s,t)$ can be decomposed into two factors:

$$\begin{cases}u(s,t)=l(s)U(t),\\v(s,t)=m(s)V(t),\\w(s,t)=n(s)W(t),\end{cases}\qquad 0\le s\le L,\ 0\le t\le T. \tag{2.5}$$

Here $l(s)$, $m(s)$, $n(s)$, $U(t)$, $V(t)$ and $W(t)$ are all C^1 functions, and $l(s)$, $m(s)$ and $n(s)$ are not identically zero. Thus, from Eq. (2.3), we can simply express the sufficient condition for which the curve C is an isogeodesic curve on the surface $\mathbf{P}(s,t)$ as

$$\begin{cases}U(t_0)=V(t_0)=W(t_0)=0,\\\dfrac{\mathrm{d}V(t_0)}{\mathrm{d}t}=0,\ \text{or } m(s)=0,\\\dfrac{\mathrm{d}W(t_0)}{\mathrm{d}t}=\text{const}\ne 0,\\n(s)\ne 0,\end{cases} \tag{2.6}$$

$t_0\in[0,T],\ 0\le s\le L.$

The factor-decomposition form possesses an evident advantage: any set of functions $l(s)$, $m(s)$, and $n(s)$ would satisfy Eq. (2.6), thus the designer can select different sets of functions $l(s)$, $m(s)$, and $n(s)$ to adjust the shape of the surface until they are gratified with the design, and the resulting surface is guaranteed to belong to the isogeodesic surface pencil with the curve C as the common geodesic.

For convenience in practice, the marching-scale functions can be further constrained to be in more restricted forms and still possess enough degrees of freedom to define a large class of isogeodesic surface pencils. Specifically, let us suppose that $u(s,t)$, $v(s,t)$ and $w(s,t)$ depend only on the parameter t, that is, in Eq. (2.5)

$$l(s)=m(s)=n(s)\equiv 1. \tag{2.7}$$

Furthermore, we can assume that $U(t)$, $V(t)$ and $W(t)$ are all cubic polynomials, defined on interval $[0,1]$. Then the sufficient conditions in Eq. (2.6) ($n(s) \equiv 1 \neq 0$) clearly become:

$$\begin{cases} U(t) = a_1(t-t_0) + a_2(t-t_0)^2 + a_3(t-t_0)^3, \\ V(t) = b_2(t-t_0)^2 + b_3(t-t_0)^3, \\ W(t) = c_1(t-t_0) + c_2(t-t_0)^2 + c_3(t-t_0)^3, \end{cases} \tag{2.8}$$

$$c_1 \neq 0,\ 0 \leq t \leq 1,\ t_0 \in [0,1],$$

where the coefficients a_i, c_i $(i = 1,2,3)$ and b_i $(i = 2,3)$ are eight arbitrary real number constants. The corresponding isogeodesic surface pencil can then be represented as a surface family controlled by these eight parameters, i.e.

$$\left\{ \mathbf{P}(s,t;a_1,a_2,a_3,b_2,b_3,c_1,c_2,c_3) \middle| \begin{matrix} a_i,b_i,c_i \in R^1 \\ c_1 \neq 0 \end{matrix} \right\}.$$

$$0 \leq s \leq L,\ 0 \leq t \leq 1$$

If $a_1 = a_2 = a_3 = b_2 = b_3 = c_2 = c_3 = 0$, but $c_1 \neq 0$, we will obtain the simplest member. The designer can adjust these parameters to produce surfaces that meet certain constraints, such as the boundary, feature lines, data points, curvatures, etc.

As an alternative to polynomials, $U(t)$, $V(t)$ and $W(t)$ can be defined as C-Bézier splines [33,34]:

$$\begin{cases} U(t) = a_1(t-t_0) + a_2[1-\cos(t-t_0)] + a_3\sin(t-t_0), \\ V(t) = b_2[1-\cos(t-t_0)] + b_3[(t-t_0) - \sin(t-t_0)], \\ W(t) = c_1(t-t_0) + c_2[1-\cos(t-t_0)] + c_3\sin(t-t_0), \end{cases}$$

$$c_1 + c_3 \neq 0,\ 0 \leq t \leq \alpha,\ t_0 \in [0,\alpha]. \tag{2.9}$$

It is a simple matter to validate that this suite of functions satisfies the conditions in Eq. (2.6). Here we also have eight parameter values. Since the bases of C-Bézier spline are $\{1, t, \cos t, \sin t; 0 \leq t \leq \alpha\}$, C-Bézier spline can represent both free form curves and conic sections without rational polynomials. Note that here α is not only the length of the parameter interval, but also a shape control parameter.

3. Surface pencil with a geodesic expressed by an arbitrary parameter

In the majority of practical cases, the parameter of a given curve is usually not its arc length. So in this section we present an algorithm for constructing an isogeodesic surface pencil from an arbitrarily parametrized geodesic. Suppose we are given a spatial parametric curve

$$C:\ \mathbf{R}(r) = (X(r), Y(r), Z(r)), \qquad 0 \leq r \leq H, \tag{3.1}$$

where the parameter r is not the arc length. The components of the Frenet frame are now defined by [9]

$$\begin{aligned} \tilde{\mathbf{T}}(r) &= \frac{\dot{\mathbf{R}}(r)}{|\dot{\mathbf{R}}(r)|}, \\ \tilde{\mathbf{B}}(r) &= \frac{\dot{\mathbf{R}}(r) \times \ddot{\mathbf{R}}(r)}{|\dot{\mathbf{R}}(r) \times \ddot{\mathbf{R}}(r)|}, \\ \tilde{\mathbf{N}}(r) &= \tilde{\mathbf{B}}(r) \times \tilde{\mathbf{T}}(r). \end{aligned} \tag{3.2}$$

When the given curve C is in the oxy plane, the following moving frame can be used:

$$\tilde{\mathbf{T}}(r) = \frac{(\dot{X}, \dot{Y}, 0)}{\sqrt{\dot{X}^2 + \dot{Y}^2}}, \qquad \tilde{\mathbf{N}}(r) = \frac{(-\dot{Y}, \dot{X}, 0)}{\sqrt{\dot{X}^2 + \dot{Y}^2}}, \tag{3.3}$$

$$\tilde{\mathbf{B}}(r) = (0,0,1).$$

The surface pencil generated from the arbitrarily parametrized geodesic $\mathbf{R}(r)$ is expressed as

$$\tilde{\mathbf{P}}(r,t) = \mathbf{R}(r) + (u(r,t), v(r,t), w(r,t)) \begin{pmatrix} \tilde{\mathbf{T}}(r) \\ \tilde{\mathbf{N}}(r) \\ \tilde{\mathbf{B}}(r) \end{pmatrix}, \tag{3.4}$$

$$0 \leq r \leq H, 0 \leq t \leq T,$$

and the necessary and sufficient conditions for which the curve $\mathbf{R}(r)$ is an isogeodesic on the surface $\tilde{\mathbf{P}}(r,t)$ can correspondingly be written as

$$\begin{cases} u(r,t_0) = v(r,t_0) = w(r,t_0) \equiv 0, \\ \phi_1(r,t_0) = \phi_3(r,t_0) \equiv 0, \quad \phi_2(r,t_0) \neq 0, \end{cases} \tag{3.5}$$

$$0 \leq r \leq H,\ 0 \leq t_0 \leq T.$$

For the case when the marching-scale functions depend only on the parameter t, the isogeodesic surface pencil becomes

$$\tilde{\mathbf{P}}(r,t) = \mathbf{R}(r) + (U(t), V(t), W(t)) \begin{pmatrix} \tilde{\mathbf{T}}(r) \\ \tilde{\mathbf{N}}(r) \\ \tilde{\mathbf{B}}(r) \end{pmatrix}, \tag{3.6}$$

$$0 \leq r \leq H,\ 0 \leq t \leq T.$$

As in Section 2, when the marching-scale functions are all cubic polynomials, the shape of a member surface in the pencil is determined by the eight constants.

4. Examples of generating simple surfaces with common geodesics

In this section we illustrate that it is possible to derive exact isogeodesic surface pencils whose members include cylinders, surfaces of revolution, and ruled surfaces, by specifying a geodesic that represents a geometric feature of the object to be designed. In other words, the parametric

definitions of the corresponding marching-scale functions can be derived exactly based on the geometric characteristics. We present four concrete examples to illustrate this viewpoint. They also serve to verify the correctness of the formulae derived in Sections 2 and 3.

4.1. Cylinder with a geodesic circular helix

In this first example, we construct an isogeodesic surface pencil in which all the surfaces share a geodesic circular helix represented as:

$$\mathbf{R}(r) = (a\cos r, a\sin r, br), \qquad a>0,\ b\neq 0,\ 0\le r<2\pi. \tag{4.1}$$

It is easy to show that

$$\tilde{\mathbf{T}}(r) = \frac{(-a\sin r, a\cos r, b)}{\sqrt{a^2+b^2}},$$

$$\tilde{\mathbf{N}}(r) = (-\cos r, -\sin r, 0),$$

$$\tilde{\mathbf{B}}(r) = \frac{(b\sin r, -b\cos r, a)}{\sqrt{a^2+b^2}}.$$

By choosing

$$U(t)=\alpha t, \qquad V(t)=0, \qquad W(t)=\beta t,$$

$$\beta\neq 0,\ 0\le t\le T,$$

and from formula (3.6), we obtain the following isogeodesic surface pencil

$$\left\{ \begin{array}{l|l} \tilde{\mathbf{P}}(r,t;\alpha,\beta) = (a\cos r, a\sin r, br) + (\alpha,0,\beta) & \\ \qquad \begin{pmatrix} -a\sin r & a\cos r & b \\ -\cos r & -\sin r & 0 \\ b\sin r & -b\cos r & a \end{pmatrix} \dfrac{t}{\sqrt{a^2+b^2}} & \begin{array}{l}\alpha\in R^1\\ \beta\in R^1\\ \beta\neq 0\end{array} \\ 0\le r\le 2\pi,\ 0\le t\le T, & \end{array} \right\},$$

which has the curve C as a common spatial geodesic. If we let its two pencil parameters be

$$\alpha = -\frac{b^2\sqrt{a^2+b^2}}{a^2}, \qquad \beta = -\frac{b\sqrt{a^2+b^2}}{a},$$

we immediately obtain a member surface

$$\left(a\cos r, a\sin r, b\left(r-\left(1+\frac{b^2}{a^2}\right)t\right)\right),$$

$$0\le r<2\pi,\ 0\le t\le T,$$

which is obviously a cylinder with radius a. This surface is shown in yellow in Fig. 3, in which $a=2$, $b=1$, $T=10$. As a comparison, if we set $\alpha=0.1$, $\beta=-1$, we obtain another member surface in the pencil as shown in green in Fig. 3. This surface is *not* a cylinder but still possesses the same geodesic circular helix. This fact conforms with the geodesic theory in differential geometry.

4.2. Surface of revolution with a geodesic circle

Let

$$\mathbf{l}(t) = (0, l_y(t), l_z(t)), \qquad 0\le t\le T, \tag{4.2}$$

be a parametric curve in the oyz plane satisfying the following conditions:

$$\mathbf{l}(t_0) = (0,a,0), \qquad \mathbf{l}'(t_0) = (0,0,b),\ \ a>0,\ b\neq 0,\ 0\le t_0\le T. \tag{4.3}$$

By revolving the curve $\mathbf{l}(t)$, as a generating curve, about the z-axis, we obtain a surface of revolution. Suppose now we are given a circle

$$\mathbf{R}(r) = (a\cos r, a\sin r, 0), \qquad a>0,\ 0\le r<2\pi. \tag{4.4}$$

We show how to select the marching-scale functions $U(t)$, $V(t)$ and $W(t)$ in terms of $l_y(t)$, $l_z(t)$ such that the surface family $\tilde{\mathbf{P}}(r,t)$ is an isogeodesic surface pencil with the circle $\mathbf{R}(r)$ as a common geodesic.

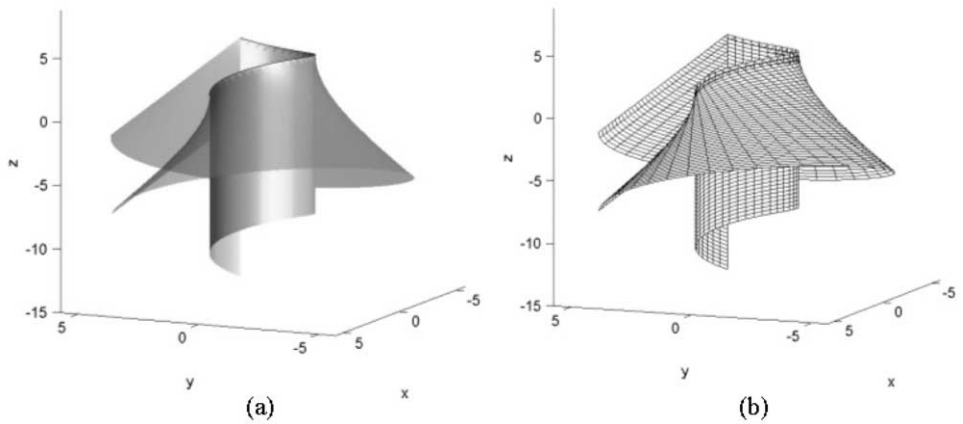

Fig. 3. Two surfaces generated with a circular helix: $\tilde{\mathbf{P}}(r,t;-\sqrt{5}/4,-\sqrt{5}/2)$ (yellow) and $\tilde{\mathbf{P}}(r,t;0.1,-1)$ (green).

It is easy to show that

$$\tilde{\mathbf{T}}(r) = (-\sin r, \cos r, 0), \qquad \tilde{\mathbf{N}}(r) = (-\cos r, -\sin r, 0),$$

$$\tilde{\mathbf{B}}(r) = (0, 0, 1).$$

Thus the surface pencil can be represented as

$$\tilde{\mathbf{P}}(r,t) = (a\cos r, a\sin r, 0) + (U(t), V(t), W(t)) \times \begin{pmatrix} -\sin r & \cos r & 0 \\ -\cos r & -\sin r & 0 \\ 0 & 0 & 1 \end{pmatrix},$$

$$0 \le r < 2\pi,\ 0 \le t \le T.$$

It follows that $\tilde{\mathbf{P}}(r,t)$ is a surface of revolution with generating curve $\mathbf{l}(t)$, i.e.

$$\tilde{\mathbf{P}}(r,t) = (l_y(t)\cos r, l_y(t)\sin r, l_z(t)),$$

if and only if

$$U(t) = 0, \quad V(t) = a - l_y(t), \quad W(t) = l_z(t),\ 0 \le t \le T.$$

This leads to the selection

$$U(t) = \alpha(t - t_0), \quad V(t) = \beta(a - l_y(t)),$$

$$W(t) = \gamma l_z(t),\ \gamma \neq 0,\ 0 \le t \le T,$$

from which it is easy to see that the functions $U(t)$, $V(t)$, and $W(t)$ comply with the conditions in Eqs. (2.5)–(2.7), given that $\mathbf{l}(t)$ satisfies the conditions in Eq. (4.3). By substituting these choices of marching-scale functions into the surface pencil equation and rearranging, we obtain the following isogeodesic surface pencil containing the common geodesic circle $\mathbf{R}(r)$:

$$\begin{cases} \tilde{\mathbf{P}}(r,t;\alpha,\beta,\gamma) = (-\alpha(t-t_0)\sin r + [a - \beta(a - l_y(t))]\cos r, \\ \qquad\qquad \alpha(t-t_0)\cos r + [a - \beta(a - l_y(t))]\sin r, \gamma l_z(t)) \\ 0 \le r < 2\pi,\ 0 \le t \le T, \end{cases}$$

Fig. 4 shows a surface of revolution (in yellow) obtained by setting $\alpha = 0$, $\beta = 1$, $\gamma = 1$, with the parametric curve $\mathbf{l}(t)$ given as

$$\mathbf{l}(t) = \left(0, a\left(\frac{2\cos t + 3}{5}\right)\left(1 - \frac{3t^2}{40}\right), bt\right),$$

$$a = 2,\ b = 1,\ t_0 = 0,\ 0 \le t < 2\pi.$$

Note that it satisfies the conditions in Eq. (4.3). We observe that when $\alpha = 0$ and $\beta \neq 1$ or $\gamma \neq 1$, the corresponding member surface is always a surface of revolution. If we choose $\alpha \neq 0$, the corresponding member surface is no longer a surface of revolution; specifically, Fig. 4 shows a surface (in green) with $\alpha = 0.3$, $\beta = 1.1$, $\gamma = 0.9$.

4.3. Surface of revolution with a geodesic as the generating curve

Suppose we are given a parametric curve in the oyz plane:

$$\mathbf{R}(r) = (0, Y(r), Z(r)), \qquad 0 \le r \le H. \tag{4.5}$$

We will construct an isogeodesic surface pencil sharing the curve $\mathbf{R}(r)$ as the geodesic, and such that a member of the pencil is a surface of revolution, on which the curve $\mathbf{R}(r)$ is not only a geodesic, but also the generating curve (which when revolved about the z-axis produces the surface of revolution).

From the definition of the Frenet frame in Eq (3.2), and denoting $D(r) = \sqrt{\dot{Y}^2(r) + \dot{Z}^2(r)}$, we obtain

$$\tilde{\mathbf{T}}(r) = (0, \dot{Y}(r), \dot{Z}(r))/D(r), \quad \tilde{\mathbf{N}}(r) = (0, -\dot{Z}(r), \dot{Y}(r))/D(r),$$

$$\tilde{\mathbf{B}}(r) = (1,0,0),\ 0 \le r \le H.$$

The isogeodesic surface pencil generated is

$$\tilde{\mathbf{P}}(r,t) = \left(w(r,t), Y(r) + \frac{u(r,t)\dot{Y}(r) - v(r,t)\dot{Z}(r)}{D(r)}, Z(r) + \frac{u(r,t)\dot{Z}(r) + v(r,t)\dot{Y}(r)}{D(r)}\right), 0 \le r \le H, 0 \le t \le T. \tag{4.6}$$

Now we consider a member of the above isogeodesic surface pencil $\tilde{\mathbf{P}}(r,t)$. If the surface is generated by rotation, its parameter t is chosen as a rotation angle, and the starting angle t_0 is equal to $\pi/2$, then it must be in the following form

$$\tilde{\mathbf{P}}(r,t) = (Y(r)\cos t, Y(r)\sin t, Z(r)),\ 0 \le r \le H, 0 \le t < 2\pi.$$

$$\left\{ \begin{array}{l} \alpha, \beta, \gamma \in R^1, \\ \gamma \neq 0 \end{array} \right\}.$$

Hence we have $w(r,t) = Y(r)\cos t$, and

$$\begin{cases} \dfrac{\dot{Y}(r)u(r,t) - \dot{Z}(r)v(r,t)}{D(r)} = Y(r)(\sin t - 1), \\ \dfrac{\dot{Z}(r)u(r,t) + \dot{Y}(r)v(r,t)}{D(r)} = 0. \end{cases} \tag{4.7}$$

Thus, suppose $\alpha(r)$, $\beta(r)$ and $\gamma(r) \neq 0$ are arbitrary three real functions, we set the marching-scale functions as

$$\begin{cases} u(r,t) = -\alpha(r)Y(r)\dot{Y}(r)(1 - \sin t)/D(r), \\ v(r,t) = \beta(r)Y(r)\dot{Z}(r)(1 - \sin t)/D(r), \\ w(r,t) = \gamma(r)Y(r)\cos t, \end{cases} \tag{4.8}$$

$$\alpha(r), \beta(r), \gamma(r) \in R^1, \gamma(r) \neq 0, 0 \le r \le H, 0 \le t < 2\pi,$$

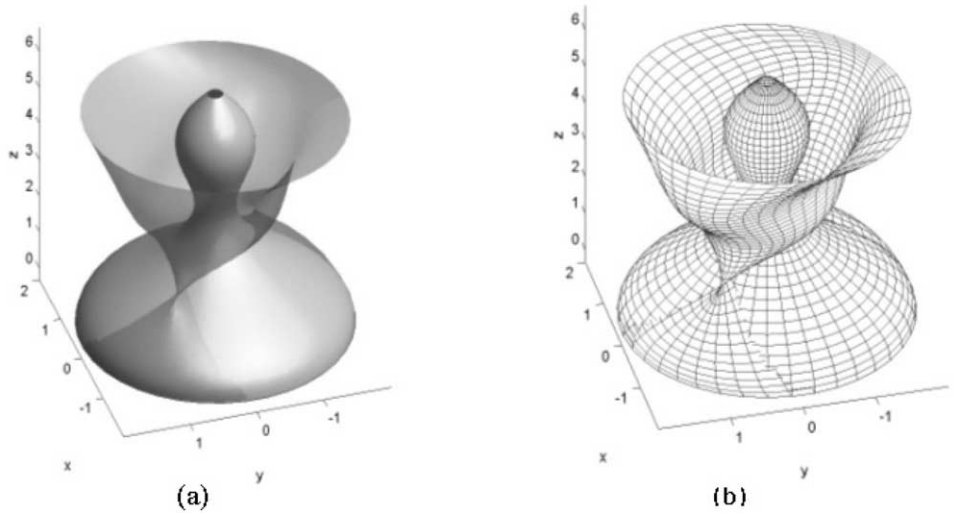

Fig. 4. Two surfaces with a common circle geodesic: $\tilde{\mathbf{P}}(r,t;0,1,1)$ (yellow) and $\tilde{\mathbf{P}}(r,t;0.3,1.1,0.9)$ (green).

to obtain the isogeodesic surface pencil

$$\{\tilde{\mathbf{P}}(r,t;\alpha(r),\beta(r),\gamma(r))|\alpha(r),\beta(r),\gamma(r)\in R^1,\gamma(r)\neq 0\}.$$

When $\alpha(r)\equiv\beta(r)\equiv\gamma(r)\equiv 1$, the functions $u(r,t)$, $v(r,t)$ and $w(r,t)$ are just the solution to system (4.7); the corresponding member surface $\tilde{\mathbf{P}}(r,t;1,1,1)=(Y(r)\cos t, Y(r)\sin t, Z(r))$ is thus also a surface of revolution.

Note that we can easily verify that the marching-scale functions satisfy the conditions for $\tilde{\mathbf{N}}(r)\|\tilde{\mathbf{n}}(r,t_0)$, $0\le r\le H$ given in Eq. (3.5) with $t_0=\pi/2$. Thus, Eqs. (4.6) and (4.8) are exactly what we are looking for.

Fig. 5 depicts two members of the isogeodesic surface pencil where the geodesic is given as

$$\mathbf{R}(r)=(0,\cos r+1.5,r),\qquad 0\le r\le 5;$$

the green and yellow surfaces have their pencil parameters set as $\alpha(r)=1$, $\beta(r)=1$, $\gamma(r)=1$ and $\alpha(r)=1.2$, $\beta(r)=1.2$, $\gamma(r)=1.8$, respectively. It is observed that the yellow surface is *not* a surface of revolution.

4.4. Ruled surface with a geodesic directrix

Ruled surfaces are an important class of surfaces widely used in many CAD systems. In this last example, we show how to derive the formulation of a ruled isogeodesic surface pencil such that the shared geodesic curve is also the directrix of the ruled surfaces. Let $\mathbf{r}(s)$ be a 3D curve where s is the arc length. Suppose $\mathbf{P}(s,t)$ is a ruled surface with the directrix $\mathbf{r}(s)$; this means that the entire surface $\mathbf{P}(s,t)$ is spanned by straight lines emanating from the curve $\mathbf{r}(s)=\mathbf{P}(s,t_0)$ going

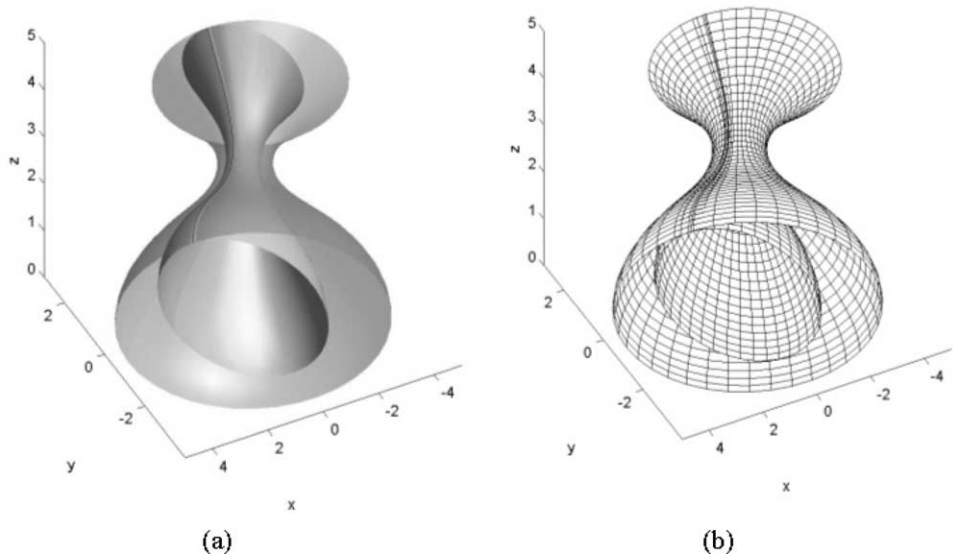

Fig. 5. Two surfaces with a geodesic generating curve: $\tilde{\mathbf{P}}(r,t;1,1,1)$ (green) and $\tilde{\mathbf{P}}(r,t;1.2,1.2,1.8)$ (yellow).

in the direction $\mathbf{D}(s)$ for some parameter t_0; that is,

$$\mathbf{P}(s,t) - \mathbf{P}(s,t_0) = (t - t_0)\mathbf{D}(s),$$

$$0 \le s \le L,\ 0 \le t \le T,\ t_0 \in [0,T].$$

From Eq. (2.2), the surface is equivalent to

$$(u(s,t), v(s,t), w(s,t))\begin{pmatrix}\mathbf{T}(s)\\ \mathbf{N}(s)\\ \mathbf{B}(s)\end{pmatrix} = (t - t_0)\mathbf{D}(s),$$

$$0 \le s \le L,\ 0 \le t \le T,\ t_0 \in [0,T].$$

Writing the above equation for each of its coordinate components, we obtain a system of three equations with three unknowns $u(s,t)$, $v(s,t)$, and $w(s,t)$. Denoting the scalar triple product of three vectors $\mathbf{a}, \mathbf{b}$, and $\mathbf{c}$ as $(\mathbf{a}, \mathbf{b}, \mathbf{c})$, their solutions can be represented as:

$$\begin{cases} u(s,t) = (\mathbf{D}(s), \mathbf{N}(s), \mathbf{B}(s))(t - t_0), \\ v(s,t) = (\mathbf{T}(s), \mathbf{D}(s), \mathbf{B}(s))(t - t_0), \\ w(s,t) = (\mathbf{T}(s), \mathbf{N}(s), \mathbf{D}(s))(t - t_0), \end{cases} \tag{4.9}$$

$$0 \le s \le L,\ 0 \le t \le T,\ t_0 \in [0,T].$$

The above equations are just the necessary and sufficient conditions for which $\mathbf{P}(s,t)$ is a ruled surface with a directrix $\mathbf{r}(s)$. Next, we need to check if the curve $\mathbf{r}(s)$ is also a geodesic on the surface $\mathbf{P}(s,t)$ by using the conditions given in Eq. (2.6). It is evident that in this case these conditions become:

$$\begin{cases} (\mathbf{T}(s), \mathbf{D}(s), \mathbf{B}(s)) = 0, \\ (\mathbf{T}(s), \mathbf{N}(s), \mathbf{D}(s)) \ne 0, \end{cases} \qquad 0 \le s \le L.$$

It follows that the at any point on the curve $\mathbf{r}(s)$, the ruling direction $\mathbf{D}(s)$ must be in the plane formed by $\mathbf{T}(s)$ and $\mathbf{B}(s)$. On the other hand, the ruling direction $\mathbf{D}(s)$ and the vector $\mathbf{T}(s)$ must not be parallel. This implies

$$\mathbf{D}(s) = \alpha(s)\mathbf{T}(s) + \beta(s)\mathbf{B}(s), \qquad \beta(s) \ne 0,\ 0 \le s \le L \tag{4.10}$$

for some real functions $\alpha(s)$ and $\beta(s)$. Substituting it into the expressions in Eq. (4.9), we get

$$u(s,t) = \alpha(s)t, \qquad v(s,t) = 0, \qquad w(s,t) = \beta(s)t,$$

$$\beta(s) \ne 0.$$

So, the isogeodesic surface pencil with the common geodesic directrix $\mathbf{r}(s)$ is given by

$$\{\mathbf{P}(s,t;\alpha,\beta) = \mathbf{r}(s) + t\alpha(s)\mathbf{T}(s) + t\beta(s)\mathbf{B}(s),\ 0 \le s \le L,\ 0 \le t \le T | \alpha, \beta \in R^1,\ \beta \ne 0\},$$

where $\alpha(s)$ and $\beta(s)$ are two controlling functions of the pencil.

It should be pointed out that in this model, there exist two geodesics passing through every point on the curve $\mathbf{r}(s)$—one is $\mathbf{r}(s)$ itself, and the other is a straight line in the direction $\mathbf{D}(s)$ as given in Eq. (4.10). Every member of the isogeodesic surface pencil is decided by two pencil parameters $\alpha(s)$ and $\beta(s)$, i.e. by the direction vector function $\mathbf{D}(s)$. Fig. 6 shows two member surfaces of a ruled isogeodesic surface pencil whose geodesic directrix is the circular helix in Eq. (4.1), with $a = 2$, $b = 1$, $T = 10$. The controlling functions of the two surfaces are $\alpha(r) = \beta(r) = \sqrt{r}$ (yellow) and $\alpha(r) = 1.3\sqrt{r}$, $\beta(r) = 1.1\sqrt{r}\sin(r/4)$ (green), respectively.

5. An application example in garment design

In this section, we demonstrate how the methodology of constructing an isogeodesic surface pencil developed in this paper can be used in garment design. A piece of garment,

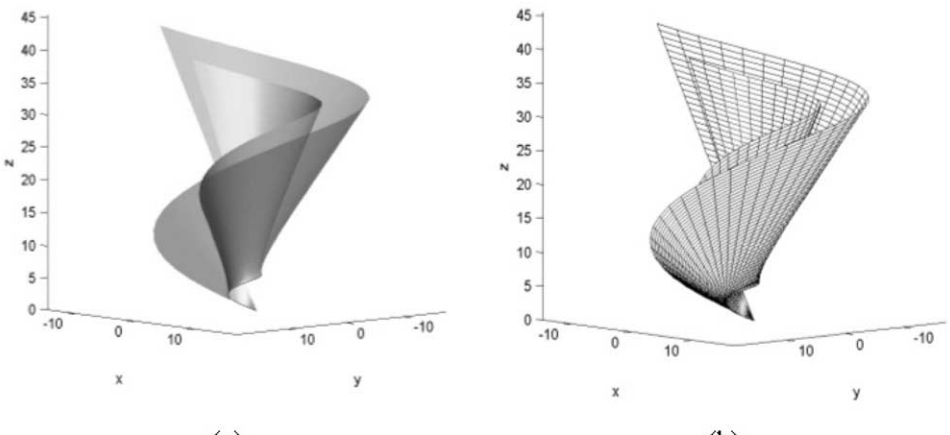

Fig. 6. Two ruled surfaces with a circular helix geodesic: $\tilde{\mathbf{P}}(r,t;\sqrt{r},\sqrt{r})$ (yellow) and $\tilde{\mathbf{P}}(r,t;1.3\sqrt{r},1.1\sqrt{r}\sin(r/4))$ (green).

such as a dress, is usually characterized by some key curves, e.g. the waist line and chest line, which are assigned measurements or dimensions. Given the nominal size of a design, these salient dimensional curves are usually fixed, while the shape of the garment itself may change to suit the design intents. Many of these key dimensional curves are required to be straight or near-straight lines when the piece of clothing is flattened into its planar counter-part. Therefore, in principle, these dimensional curves are preferred to be geodesics on the surface of the garment. Fig. 7 shows a dress with its waist line marked in black; here the waist line happens to be a planar curve but it need not be so in general.

We now apply the concept of isogeodesic surface pencil to the design of a dress. Assume that we are given a mesh model for the dress. This initial model could be obtained from some existing sample via laser scanning or based on some conceptual designs. Also assume that the waist line is the only key dimensional curve, represented as a 3D B-spline curve $\mathbf{R}(r)$ embedded on the given model. Basically, we want to model the dress as an isogeodesic surface with $\mathbf{R}(r)$ as a geodesic. The initial model can be thought of as a *reference design*. The objective is to find the 'nominal' values—$a_1^*, a_2^*, a_3^*, b_2^*, b_3^*, c_1^*, c_2^*, c_3^*$—of the eight parameters so that the corresponding member surface (as defined by Eqs. (3.6) and (2.8)) contains $\mathbf{R}(r)$ as a geodesic and closely approximates this reference design. Once these nominal parameters are determined, the designer can then change the eight parameters around these values to modify the shape of the dress, while having the comfort that, no matter what values the parameters take, the corresponding surface always has $\mathbf{R}(r)$ as a geodesic.

To find these nominal parameter values, we employ the least square fitting method. Specifically, the initial model is sampled to obtain a set of data points $\{\mathbf{Q}_{i,j}\}_{i=1\ j=1}^{m,n} \in R^3$, capturing the important characteristics such as the boundary and other critical points. We assume that the data points are sampled in a sectional fashion; that is, the points in the ith row $\{\mathbf{Q}_{i,j}\}_{j=1,2,\ldots,n}$ lie on a plane parallel to the curve $\mathbf{R}(r)$, and they are ordered in the row from 'left' to 'right'. The waist line $\mathbf{R}(r)$ divides the surface of the model into two regions: S_{lower} and S^{upper}. Let the first k rows be in S_{lower} and the rest of the rows be in S^{upper}. Let the parameter range for the surface $\tilde{\mathbf{P}}(r,t)$ be $[0,H]\times[0,1]$. A simple parameterization scheme for the two regions S^{upper} and S_{lower} is suggested as follows:

$$\mathbf{Q}_{i,j} \leftrightarrow (r_j, t_i), \qquad i = 1,2,\ldots,m;\ j = 1,2,\ldots,n;$$

$$r_j = \frac{H\sum_{\eta=1}^{j-1}\|\mathbf{Q}_{i,\eta+1}-\mathbf{Q}_{i,\eta}\|}{\sum_{\eta=1}^{n-1}\|\mathbf{Q}_{i,\eta+1}-\mathbf{Q}_{i,\eta}\|}, \qquad j = 1,2,\ldots,n;$$

$$t_i = \begin{cases} 0.5\times\left(\dfrac{\sum_{\xi=1}^{i-1}\|\mathbf{Q}_{\xi+1,j}-\mathbf{Q}_{\xi,j}\|}{\sum_{\xi=1}^{k-1}\|\mathbf{Q}_{\xi+1,j}-\mathbf{Q}_{\xi,j}\|}\right), & \text{if } i \le k \\ 0.5\times\left(1+\dfrac{\sum_{\xi=k+1}^{i-1}\|\mathbf{Q}_{\xi+1,j}-\mathbf{Q}_{\xi,j}\|}{\sum_{\xi=k+1}^{m-1}\|\mathbf{Q}_{\xi+1,j}-\mathbf{Q}_{\xi,j}\|}\right), & \text{if } i > k \end{cases},$$

$$i = 1,2,\ldots,m.$$

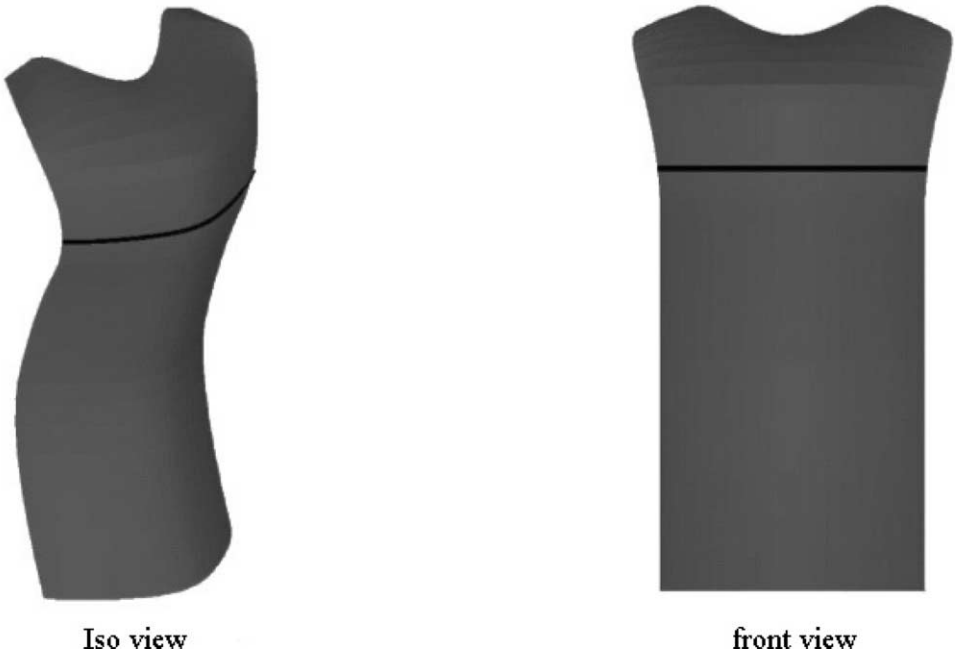

Fig. 7. The original model of a dress and its waist line.

Fig. 8. Nominal isogeodesic surface with its parameters.

Note that, with this parameter assignment, the parameter for the curve $\mathbf{R}(r)$ is $t_0 = 0.5$. Introducing a variable g to iterate through the x, y, z coordinates of the various vector functions, the cost function of the approximation can be expressed as

$$F(a_1, a_2, a_3, b_2, b_3, c_1, c_2, c_3) = \sum_{i=1}^{m}\sum_{j=1}^{n} \|\tilde{P}(r_j, t_i) - Q_{i,j}\|^2$$
$$= \sum_{i=1}^{m}\sum_{j=1}^{n}\sum_{g=x,y,z} [R_g(r_j) + (U(t_i)\tilde{T}_g(r_j) + V(t_i)\tilde{N}_g(r_j) + W(t_i)\tilde{B}_g(r_j)) - (Q_g)_{i,j}]^2,$$

where $U(t_i)$, $V(t_i)$, $W(t_i)$ and $\tilde{T}_g(r_j)$, $\tilde{N}_g(r_j)$, $\tilde{B}_g(r_j)$, $g = x, y, z$, can be computed by Eqs. (2.8) and (3.2), respectively. To minimize this cost function, its partial derivatives with respect to the variable parameters are set to zero. Thus, we obtain a system of linear equations in the eight variables, a_1, a_2, a_3, b_2, b_3, c_1, c_2 and c_3 :

$$\frac{\partial F}{\partial a_l} = \sum_{i=1}^{m}\sum_{j=1}^{n}\left((t_i - t_0)^l \sum_{g=x,y,z} \tilde{T}_g(r_j)\right)[R_g(r_j) + (U(t_i)\tilde{T}_g(r_j) + V(t_i)\tilde{N}_g(r_j) + W(t_i)\tilde{B}_g(r_j)) - (Q_g)_{i,j}]$$
$$= 0,$$

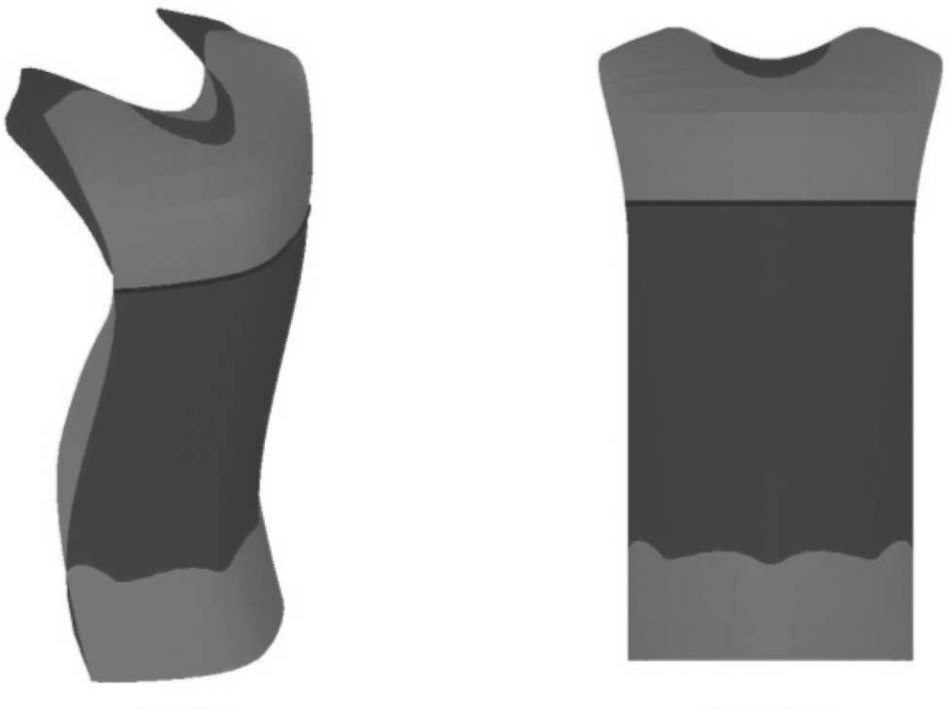

Fig. 9. The superimposed original (purple) and the nominal isogeodesic (blue) surfaces.

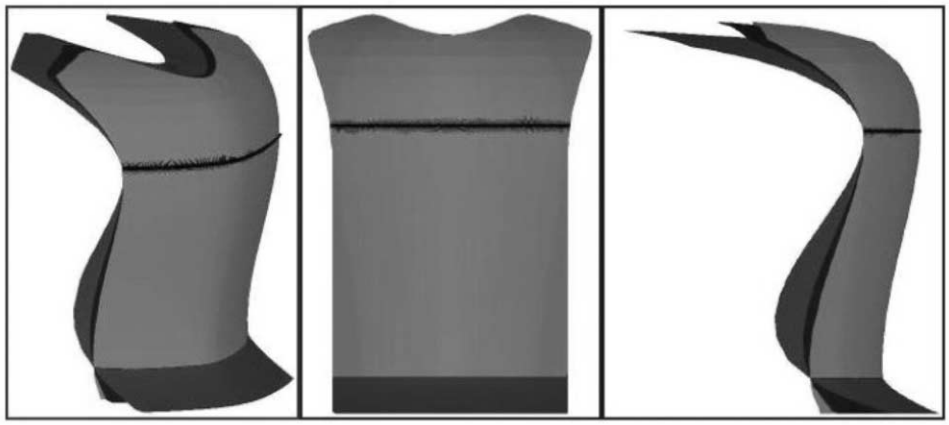

Blue(nominal)	Red	Green
a_1^*	a_1^*	a_1^*
a_2^*	a_2^*	a_2^*
a_3^*	a_3^*	a_3^*
b_2^*	b_2^*+***abs***(b_2^*)*0.1	b_2^*-***abs***(b_2^*)*0.1
b_3^*	b_3^*+***abs***(b_3^*)*0.1	b_3^*-***abs***(b_3^*)*0.1
c_1^*	c_1^*+***abs***(c_1^*)*0.1	c_1^*-***abs***(c_1^*)*0.1
c_2^*	c_2^*+***abs***(c_2^*)*0.1	c_2^*-***abs***(c_2^*)*0.1
c_3^*	c_3^*+***abs***(c_3^*)*0.1	c_3^*-***abs***(c_3^*)*0.1

Fig. 10. Three members of an isogeodesic surface pencil.

$$\frac{\partial F}{\partial b_h} = \sum_{i=1}^{m}\sum_{j=1}^{n}\left((t_i - t_0)^h \sum_{g=x,y,z} \tilde{N}_g(r_j)\right)[R_g(r_j) + (U(t_i)\tilde{T}_g(r_j) + V(t_i)\tilde{N}_g(r_j) + W(t_i)\tilde{B}_g(r_j)) - (Q_g)_{i,j}] = 0,$$

$$\frac{\partial F}{\partial c_k} = \sum_{i=1}^{m}\sum_{j=1}^{n}\left((t_i - t_0)^k \sum_{g=x,y,z} \tilde{B}_g(r_j)\right)[R_g(r_j) + (U(t_i)\tilde{T}_g(r_j) + V(t_i)\tilde{N}_g(r_j) + W(t_i)\tilde{B}_g(r_j)) - (Q_g)_{i,j}] = 0,$$

$l = 1,2,3;\ h = 2,3;\ k = 1,2,3.$

The solutions to the above system of equations—a_1^*, a_2^*, a_3^*, b_2^*, b_3^*, c_1^*, c_2^*, c_3^*—are the nominal parameters sought. The corresponding surface closely approximates the initial model and at the same time possesses curve $\mathbf{R}(r)$ as a geodesic. By changing the values of the eight parameters around their nominal values, one can achieve different designs for the dress, all of which share the same geodesic waist line $\mathbf{R}(r)$.

As an illustration, the nominal isogeodesic surface $\tilde{\mathbf{P}}(r, t, a_1^*, a_2^*, a_3^*, b_2^*, b_3^*, c_1^*, c_2^*, c_3^*)$ that approximates the original reference model of Fig. 7 is shown in Fig. 8; for comparison purpose, it is also shown in Fig. 9 superimposed with the original reference surface. Three variations of the design surface are shown in Fig. 10, with one being the nominal and the other two obtained by deviating the nominal parameter values $\{b_2^*, b_3^*, c_1^*, c_2^*, c_3^*\}$ by certain amounts. We point out that in this particular example the three parameters a_1, a_2, and a_3 are kept unchanged, as the original model is symmetric about its center line and it is found that changes of these three parameters from their nominal values will alter this symmetry.

6. Conclusion

We have presented a method for finding a surface pencil whose members all share a given geodesic curve as an isoparametric curve. The surface pencil is controlled by three marching-scale functions. For the simpler case when

the marching-scale functions are univariate and cubic, the surface pencil is parameterized by eight constants. We verify the method by finding exact surface pencil formulations whose members include simple surfaces that are commonly used in CAD. To illustrate potential applications of our method, we show how to find the surface pencil representation for surfaces of more general object models. Least square fitting is employed to fit the surface of the given model and the resulting linear system is solved for the values of the eight parameters. These values can then be perturbed to achieve variations in the design surface, which are guaranteed to produce surfaces that contain the given geodesic.

Several open issues remain. While requiring the shared geodesic to be an isoparametric curve on the surface greatly simplifies the derivation and analysis of the formulae, the constraint nevertheless limits the domain of surfaces sharing the same geodesic curve. One possible alternative is to consider the realm of implicit surfaces $F(X,Y,Z)=0$ and attempt to establish the conditions for a given parametric curve $\mathbf{r}(s)$ to be a geodesic on $F(X,Y,Z)=0$. Another possibility is that, while still requiring the surface to be parametric, the curve $\mathbf{r}(s)$ does not have to be isoparametric on the parametric surface $\tilde{\mathbf{P}}(r,t)$, but instead is related to $\tilde{\mathbf{P}}(r,t)$ by an algebraic constraint; that is, $\mathbf{r}(s)=\tilde{\mathbf{P}}(r(s),t(s))$ where $r(s)$ and $t(s)$ are two pre-specified algebraic functions. A further relaxation is to allow multiple geodesics: given m parametric curves $\mathbf{r}_i(s)$ and $2m$ smooth algebraic functions $r_i(s)$ and $t_i(s)$, $i=1,2,\ldots,m$, find a geodesic surface pencil $\tilde{\mathbf{P}}(r,t)$ such that $\mathbf{r}_i(s)=\tilde{\mathbf{P}}(r_i(s),t_i(s))$ and $\mathbf{r}_i(s)$, $i=1,2,\ldots,m$, are geodesics on $\tilde{\mathbf{P}}(r,t)$.

Acknowledgments

The first author was supported by the NNSF of China, the NNSF for IRG (No. 60021201) and the 973 Item (No. 2002CB312101). The authors thank Mr Ming Lok Yeung in the Department of Mechanical Engineering at Hong Kong University of Science and Technology for his implementation work that contributes to Section 5.

References

[1] Agarwal PK, Har-Peled H, Sharir M, Varadarajan K. Approximating shortest paths on a convex polytope in three dimensions. J. ACM 1997;44:567–84.
[2] Azariadis PN, Aspragathos NA. Geodesic curvature preservation in surface flattening through constrained global optimization. Comput-Aided Des 2001;33:581–91.
[3] Azariadis P, Aspragathos NA. Design of plane developments of doubly curved surfaces. Comput-Aided Des 1997;29(10):675–85.
[4] Brond R, Jeulin D, Gateau P, Jarrin J, Serpe G. Estimation of the transport properties of polymer composites by geodesic propagation. J Microsc 1994;176:167–77.
[5] Bryson S. Virtual spacetime: an environment for the visualization of curved spacetimes via geodesic flows. Technical Report, NASA NAS, Number RNR-92-009; March 1992.
[6] Caselles V, Kimmel R, Sapiro G. Geodesic active contours. Int J Comput Vision 1997;22(1):61–79.
[7] Cohen L, Kimmel R. Global minimum for active contours models: a minimal path approach. Int J Comput Vision 1997;24(1):57–78.
[8] Chazelle B, Edelsbrunner H, Grigni M, Guibas L, Hershberger J, Sharir M, Snoeyink J. Ray shooting in polygons using geodesic triangulations automata. Languages and programming, 18th International Colloquium. Lecture notes in computer science, vol. 510, Berlin: Springer; 1991. p. 646–661.
[9] Farin G. Curves and surfaces for computer aided geometric design, 2nd ed. New York: Academic Press; 1990.
[10] Faux ID, Pratt MJ. Computational geometry for design and manufacturing. England: Ellis Horwood; 1979.
[11] Goldenberg R, Kimmel R, Rivlin E, Rudzsky M. Fast geodesic active contours. IEEE Trans Image Process 2001;10(10):1467–75.
[12] Grundig L, Ekert L, Moncrieff E. Geodesic and semi-geodesic line algorithms for cutting pattern generation of architectural textile structures. In: Lan TT, editor. Proceedings of the Asia-Pacific Conference on Shell and Spatial Structures, Beijing. 1996.
[13] Har-Peled H. Approximate shortest paths and geodesic diameter on a convex polytope in three dimensions. GEOMETRY: discrete and computational geometry, vol. 21; 1999.
[14] Haw RJ. An application of geodesic curves to sail design. Comput Graphics Forum 1985;4(2):137–9.
[15] Haw RJ, Munchmeyer RC. Geodesic curves on patched polynomial surfaces. Comput Graphics Forum 1983;2(4):225–32.
[16] Heikes R, Randall DA. Numerical integration of the shallow-water equations of a twisted icosahedral grid. Part I: basic design and results of tests. Mon Weath Rev 1995;123:1862–80.
[17] Heikes R, Randall DA. Numerical integration of the shallow-water equations of a twisted icosahedral grid. Part II: a detailed description of the grid and an analysis of numerical accuracy. Mon Weath Rev 1995;123:1881–7.
[18] Kass M, Witkin A, Terzopoulos D. Snakes: active contour models. Int J Comput Vision 1988;1(4):321–31.
[19] Kimmel R, Amir A, Bruckstein AM. Finding shortest paths on surfaces. Presented in Curves and Surfaces, Chamonix, France, June 1993. In: Laurent, Le. Méhauté, Schumaker, editors. Curves and surfaces in geometric design; 1994. p. 259–68.
[20] Kimmel R, Amir A, Bruckstein AM. Finding shortest paths on surfaces using level sets propagation. IEEE Trans PAMI 1995;17(1):635–40.
[21] Kimmel R, Kiryati N. Finding shortest paths on surfaces by fast global approximation and precise local refinement. Int J Pattern Recogn Artif Intell 1996;10(6):643–56.
[22] Kimmel R. Intrinsic scale space for images on surfaces: the geodesic curvature flow. Graphical Models Image Process 1997;59(5):365–72.
[23] Kimmel R, Sethian JA. Computing geodesic paths on manifolds. Proceedings of National Academy of Sciences 1998;95(15):8431–5.
[24] Kimmel R, Sethian JA. Fast marching methods for computing distance maps and shortest paths. CPAM Report 669. Berkeley: University of California; 1996.
[25] Kimmel R, Kiryati N, Bruckstein AM. Multi-valued distance maps in finding shortest paths between moving obstacles. IEEE Trans Robot Automat 1998;14(3):427–36.
[26] Kimmel R, Malladi R, Sochen N. Images as embedded maps and minimal surfaces: movies, color, texture, and volumetric medical images. Int J Comput Vision 2000;39(2):111–29.
[27] Lantuejoul C, Maisonneuve F. Geodesic methods in quantitative image analysis. Pattern Recogn 1984;17:177–87.
[28] Lindeberg T. Scale-space theory in computer vision. Dordrecht: Kluwer Academic; 1994.
[29] Novotni M, Klein R. Computing geodesic paths on triangular meshes. J WSCG 2002;10.
[30] Polthier K, Schmies M. Straightest geodesics on polyhedral surfaces. In: Hege HC, Polthier K, editors. Mathematical visualization. Berlin: Springer; 1998. ISBN 3-540-63991-8.

[31] Spivak M. A comprehensive introduction to differential geometry, 2nd ed. Houston: Publish or Perish; 1979.
[32] ToiVanen PJ. New geodesic distance transforms for gray-scale images. Pattern Recogn Lett 1996;17(5):437–50.
[33] Zhang JW. C-curves: an extension of cubic curves. Comput Aided Geom Des 1996;13(3):199–217.
[34] Zhang JW. C-Bézier curves and surfaces. Graphical Models Image Process 1999;61(1):2–15.
[35] Williamson DL. Integration of the barotropic vorticity equation on a spherical geodesic grid. Tellus 1968;20:642–53.

Guo-Jin Wang is a professor and supervisor of doctoral student in the Department of Mathematics and the Institute of Computer Images and Graphics, Zhejiang University, Hangzhou, China. He received his BSc and MSc in Mathematics from Zhejiang University. His teaching and research activities are concerned with applied mathematics, computer aided geometric design, computer graphics and geometric modeling. Between 1991 and 1993, he was a visiting researcher at Brigham Young University, USA. He also was a visiting researcher at Hong Kong University of Science and Technology, in 2001 and 2003. He has published numerous papers on CAGD and CG, and is the co-author of the book, CAGD, published by China Higher Education Press, Beijing and Springer-Verlag, Berlin, Heidelberg.

Tang is currently a faculty member in the Department of Mechanical Engineering at Hong Kong University of Science and Technology. Before joining HKUST in 2001, he had worked for more than 13 years in the CAD/-CAM and IT industries. His research interests concentrate on designing efficient and practical algorithms for solving real world computational, geometric, and numerical problems. Dr Tang received PhD in Computer Engineering from the University of Michigan in 1990, MSc in Information and Control Engineering in 1986 also from the University of Michigan, and BSc in Mechanical Engineering from Nanjing Institute of Technology in China in 1982.

Chiew-Lan Tai is currently an Assistant Professor at the Computer Science Department, Hong Kong University of Science and Technology. She received her BSc and MSc in Mathematics from the University of Malaya, her MSc in Computer and Information Sciences from the National University of Singapore, and her DSc in Information Science from the University of Tokyo. Her research interests include geometric modeling and computer graphics.